Modeling Sonic Boom Propagation Through Planetary Boundary Layer Turbulence near the Lateral Extent of the Carpet

Alexander N. Carr, [1] Joel B. Lonzaga, [2] and Steven A. E. Miller [1]

[1]Mechanical and Aerospace Engineering, University of Florida, Gainesville, Fl.

[2]Structural Acoustics Branch, NASA Langley Research Center, Hampton, VA, United States.

December 10, 2020

Acknowledgements

- The first author would like to acknowledge the NASA Fellowships management team, NASA Commercial Supersonic Technology Project and the NASA Langley Structural Acoustics Branch for supporting this work. Grant number: 80NSSC19K1685

Current Shortcomings

- QSF18 reports of booms heard outside the predicted carpet
- Traditional ray theory codes cannot make predictions in the shadow zone
- Consequences:
  - Computational prediction datasets are incomplete
  - Decisions about community response testing area based on narrow carpet predictions

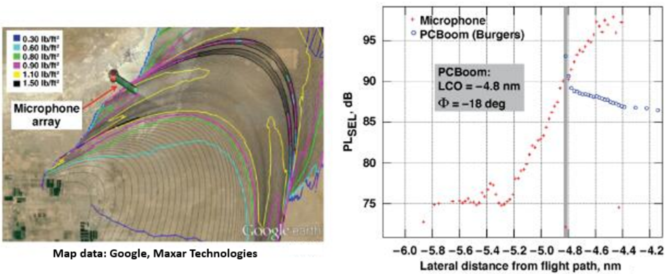

Figure 1: Perceived Sound Exposure level at the lateral extent of the carpet (Cliatt et al. [1]) compared with PCBoom predictions. Both figures from Cliatt et al. [1].

Objectives of the Research

- Develop an efficient code suitable for parallel computing to predict the effects of turbulence and ground diffraction on sonic boom
- Relate parameters of turbulence to waveform characteristics
- Predict the falloff in the loudness level at the edge of the sonic boom carpet.

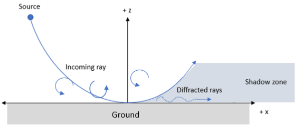

Figure 2: Diagram of diffraction process between incoming ray and ground

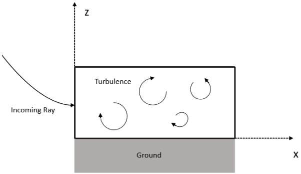

Figure 3: Illustration of the computational domain of the code.

FLHOWARD Equation I

- Coulouvrat [2] performed a decomposition on the N-S equations. Each variable can be decomposed into the acoustic component $\tilde{q}$ and flow component $\breve{q}$,

$$q(x_i, t) = \tilde{q}(x_i, t) + \breve{q}(x_i), \tag{1}$$

$$\breve{q}(x_i) = \overline{q}(x_3) + q'(x_i). \tag{2}$$

- $u_i'(x_i)$ are the velocity fluctuations, $c'(x_i)$ and $\rho'(x_i)$ are related to temperature fluctuations. The governing equation becomes,

$$\frac{1}{\breve{c}^2}\frac{\overline{D}^2\tilde{p}}{\overline{D}t^2} - \breve{\rho}\frac{\partial}{\partial x_i}\left(\frac{1}{\breve{\rho}}\frac{\partial \tilde{p}}{\partial x_i}\right) + 2\frac{\partial \overline{u}_j}{\partial x_3}\int_{-\infty}^{t}\frac{\partial^2 \tilde{p}}{\partial x_3 \partial x_j}dt' = -\frac{2}{\breve{c}^2}u_i'\frac{\partial}{\partial t}\left(\frac{\partial \tilde{p}}{\partial x_i}\right) + \frac{\beta}{\breve{\rho}\breve{c}^4}\frac{\partial^2 \tilde{p}^2}{\partial t^2} + \frac{\delta}{\breve{c}^4}\frac{\partial^3 \tilde{p}}{\partial t^3} + O(\epsilon^3, \epsilon M^3). \tag{3}$$

FLHOWARD Equation II

- Molecular relaxation is not included in Eqn. 3, but is incorporated in the absorption computation.
- Luquet [3] applies a wide-angle parabolic approximation to the heterogeneous terms. A partially one-way equation for the pseudo-potential can then be written,

$$\frac{\partial^2 \phi}{\partial x \partial \tau} = D\phi + H\phi + N\phi + A\phi. \tag{4}$$

- D = Diffraction term, H = Heterogeneous terms, N = Nonlinearities and A = absorption term
- Neglecting D and H reduces Eqn. 4 to Burgers equation of PCBoom [4]

$$D\phi = \frac{\overline{c}}{2}\Delta\phi, \qquad N\phi = \frac{\beta}{2\overline{\rho c}^3}\frac{\partial}{\partial \tau}\left(\frac{\partial \phi}{\partial \tau}\right)^2, \qquad A\phi = \frac{\partial}{\partial \tau}\left(\frac{\delta}{2\overline{c}^3}\frac{\partial^2 \phi}{\partial \tau^2}\right)$$

Benchmark Problems I

- Benchmark cases:
  1. Diffraction by a circular aperture of radius 4λ
  2. Scattering by a spherical temperature heterogeneity of radius λ
  3. Nonlinear propagation of a sinusoidal wave
  4. Absorption effects on nonlinear propagation (Mendousse [5])
- Diffraction: Angular spectrum method to compute forward solution of $\frac{\partial^2 \phi}{\partial x \partial \tau} = \frac{\bar{c}}{2} \Delta \phi$
- Sphere: 5% increase in the sound speed $c = c_0 + 0.05 c_0 \mathrm{rect}\left(\frac{r}{2\lambda}\right)$

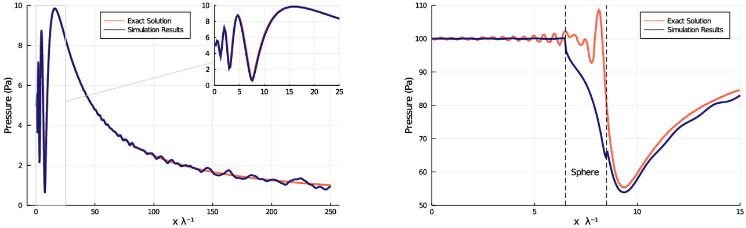

(a) Circular aperture

(b) Sphere

Figure 4: Centerline profiles along the propagation direction for both the diffraction benchmark problem (a) and the spherical heterogeneity (b).

Benchmark Problems II

- Propagation of a sinusoidal wave in a quiescent medium
- Amplitude large enough to cause nonlinear distortion of the wave
- Solve Burgers equation and compare solution to Blackstock Bridging Function [6]

- Absorption coefficient α incorporates molecular relaxation and thermoviscous effects [7]

$$\tilde{\phi}(x + \Delta x, \omega) = \tilde{\phi}(x, \omega) e^{-\alpha(\omega)\Delta x} \quad (5)$$

- Absorption can be tested with problem of Mendousse [5]

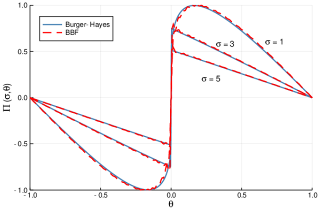

(a) Nonlinear wave propagation

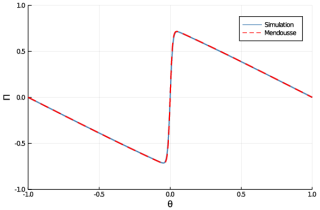

(b) Nonlinear wave propagation with absorption

Figure 5: Waveform computed at different propagation distances compared to the Blackstock bridging function [6]. Π is the normalized pressure $P/P_{max}(\sigma = 0)$, σ is the shock formation distance, and $\theta = \tau/\omega$ (a). Comparison to Mendousse solution at $\sigma = 3$ (b)

Monin-Obuhkov Similarity Theory

- Measurements of velocity and temperature profiles in the atmospheric boundary layer are not abundant
- It is desirable to model the fluid dynamics in the computational domain with nondimensional parameters
- Model mean quantities u and T with similarity theory
- Following Wilson 2001 [8]:

$$u(z) = \frac{u_*}{\kappa_v}\left[ln\left(\frac{z}{z_0}\right) - \psi_m\left(\frac{z}{L_0}\right) + \psi_m\left(\frac{z_0}{L_0}\right)\right] \tag{6}$$

$$T(z) = T_r - (z - z_r)\Gamma_d + \frac{P_t T_*}{\kappa_v}\left[ln\left(\frac{z}{z_r}\right) - \psi_h\left(\frac{z}{L_0}\right) + \psi_h\left(\frac{z_r}{L_0}\right)\right] \tag{7}$$

- ψ functions chosen to have correct asymptotic behavior for $z/L_0 \longrightarrow -\infty$ (free convection)

Comparison with Measurements

- SODAR data measured at AFRC
- Data is nondimensionalized according to Monin and Obukhov [9]
- Black lines represent prediction of M-O similarity theory
- For visualization purposes, negative ξ values are normalized by 10

$$\xi = \frac{z}{L_0}$$

$$u* = \sqrt{\frac{\tau}{\rho}}$$

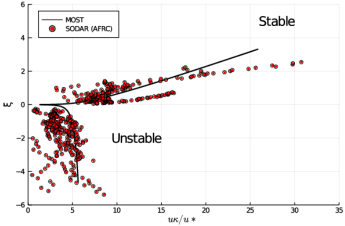

Figure 6: SODAR data taken at AFRC plotted against the universal function for Monin-Obukhov similarity theory given by [8]

Artificial Construction of Turbulent Field I

- Frelich et al. [10] spectral domain algorithm to generate turbulent field
- $\mathbf{u}$ is computed from the inverse Fourier transform of $\mathbf{w}$

$$\mathbf{u}(\mathbf{x}, t) = Re\left[\int_{-\infty}^{\infty} \mathbf{w}(\mathbf{k}, t)\, e^{i\mathbf{k}\cdot\mathbf{x}} d\mathbf{k}.\right] \tag{8}$$

- $\mathbf{w}$ determined from composite model spectrum

$$\begin{bmatrix} w_1 \\ w_2 \\ w_3 \end{bmatrix} = \begin{bmatrix} H_{11} & 0 & 0 \\ H_{12} & H_{22} & 0 \\ H_{13} & H_{23} & H_{33} \end{bmatrix} \begin{bmatrix} N_1 \\ N_2 \\ N_3 \end{bmatrix} \tag{9}$$

- $\mathbf{N}$ is a complex Gaussian random number. $\mathbf{H}$ is determined from von Kármán spectral model. Indices represent cartesian coordinates (x_1, x_2, x_3).
- Example for H_{11}, where F_{11} is the longitudinal model spectrum

$$H_{11} = \sqrt{F_{11}(k_1, k_2, k_3)\Delta k_1, \Delta k_2, \Delta k_3} \tag{10}$$

Artificial Construction of Turbulent Field II

- Compare results with the wind tunnel grid turbulence case of Comte-Bellot and Corrsin [11]

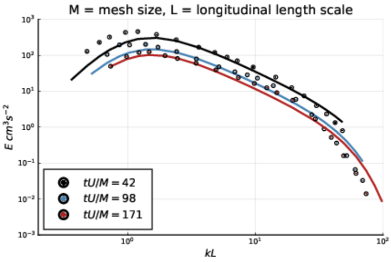

(a) Turbulent kinetic energy spectrum

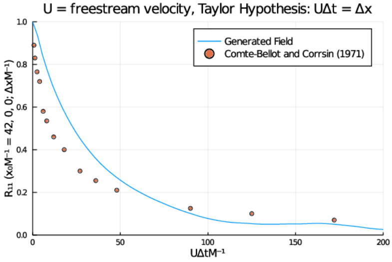

(b) Autocorrelation

Figure 7: von Kármán composite energy spectrum compared to the measurement and the Autocorrelation of the numerically generated field compared to measurements of Comte-Bellot and Corrsin [11].

Conclusions and Going Forward

- Conclusions
  - A prediction tool is being developed that accounts for diffraction, scattering, absorption and nonlinear propagation
  - Similarity theory and a model for the turbulent fluctuations are used to generate velocity and temperature in the computational domain
  - The mean velocity profiles and correlations of the reconstructed turbulent field match experimental data
- Future work
  - Predictions for N-wave and low boom waveforms in a realistic atmosphere
  - Comparison to current prediction codes like PCBoom
  - Ground boundary conditions and PML layers
  - Predictions with atmospheric turbulence, relating waveform characteristics to turbulence parameters

Thank you

References I

[1] L. J. Cliatt, M. A. Hill, and E. Haering, "Mach cutoff analysis and results from NASA farfield investigation of no-boom thresholds," in *22nd AIAA/CEAS Aeroacoustics Conference*, American Institute of Aeronautics and Astronautics, May 2016.

[2] F. Coulouvrat, "New equations for nonlinear acoustics in a low mach number and weakly heterogeneous atmosphere," *Wave Motion*, vol. 49, pp. 50–63, Jan. 2012.

[3] D. Luquet, *3D simulation of acoustical shock waves propagation through a turbulent atmosphere. Application to sonic boom*. Theses, Université Pierre et Marie Curie - Paris VI, Jan. 2016.

[4] J. B. Lonzaga, "Recent enhancements to NASA's PCBoom sonic boom propagation code," in *AIAA Aviation 2019 Forum*, American Institute of Aeronautics and Astronautics, June 2019.

[5] J. S. Mendousse, "Nonlinear dissipative distortion of progressive sound waves at moderate amplitudes," *The Journal of the Acoustical Society of America*, vol. 25, pp. 51–54, Jan. 1953.

[6] D. T. Blackstock, "Connection between the fay and fubini solutions for plane sound waves of finite amplitude," *The Journal of the Acoustical Society of America*, vol. 39, pp. 1019–1026, June 1966.

[7] H. E. Bass, L. C. Sutherland, A. J. Zuckerwar, D. T. Blackstock, and D. M. Hester, "Atmospheric absorption of sound: Further developments," *The Journal of the Acoustical Society of America*, vol. 97, no. 1, pp. 680–683, 1995.

[8] D. K. Wilson, "An alternative function for the wind and temperature gradients in unstable surface layers," *Boundary-Layer Meteorology*, vol. 99, pp. 151–158, Apr. 2001.

[9] A. S. Monin and A. M. Obukhov, "Basic laws of turbulent mixing in the surface layer of the atmosphere," 1954.

[10] R. Frehlich, L. Cornman, and R. Sharman, "Simulation of three-dimensional turbulent velocity fields," *Journal of Applied Meteorology*, vol. 40, pp. 246–258, Feb. 2001.

[11] G. Comte-Bellot and S. Corrsin, "Simple eulerian time correlation of full-and narrow-band velocity signals in grid-generated, 'isotropic' turbulence," *Journal of Fluid Mechanics*, vol. 48, pp. 273–337, July 1971.